



HAL
open science

AB-INITIO CALCULATION OF THE MICROSCOPIC PROPERTIES OF A GRAIN BOUNDARY IN GERMANIUM

M. Payne, P. Bristowe, J. Joannopoulos

► **To cite this version:**

M. Payne, P. Bristowe, J. Joannopoulos. AB-INITIO CALCULATION OF THE MICROSCOPIC PROPERTIES OF A GRAIN BOUNDARY IN GERMANIUM. *Journal de Physique Colloques*, 1988, 49 (C5), pp.C5-151-C5-155. 10.1051/jphyscol:1988512 . jpa-00228009

HAL Id: jpa-00228009

<https://hal.science/jpa-00228009>

Submitted on 4 Feb 2008

HAL is a multi-disciplinary open access archive for the deposit and dissemination of scientific research documents, whether they are published or not. The documents may come from teaching and research institutions in France or abroad, or from public or private research centers.

L'archive ouverte pluridisciplinaire **HAL**, est destinée au dépôt et à la diffusion de documents scientifiques de niveau recherche, publiés ou non, émanant des établissements d'enseignement et de recherche français ou étrangers, des laboratoires publics ou privés.

AB-INITIO CALCULATION OF THE MICROSCOPIC PROPERTIES OF A GRAIN BOUNDARY IN GERMANIUM

M.C. PAYNE⁽¹⁾, P.D. BRISTOWE and J.D. JOANNOPOULOS

Massachusetts Institute of Technology, Cambridge, MA 02139, U.S.A.

Abstract - An application of the molecular dynamics simulated annealing method for performing total energy calculations is made to the study of the microscopic structure of a high-angle grain boundary in germanium. In particular, two low energy $\Sigma=5$ (001) twist boundary structures are identified and their detailed bonding geometry is analysed by determining the local distribution of valence electron charge density. The structures are shown to exhibit two intrinsic defects: four-membered rings and three-fold coordinated atoms.

1. Introduction - The microscopic characterisation of grain boundaries in polycrystalline semiconductors has become essential to our understanding of the physical properties of these technologically important materials. From a theoretical standpoint, this requires a formal quantum mechanical treatment of the total energy of the grain boundary core region which should properly take into account the redistribution of electron charge density and the unrestricted relaxation of the ions. First principles approaches to calculating the total energy of solids have begun to be applied to grain boundaries in semiconductors and metals (1-3). However, the methods employed in these studies have not been entirely *ab initio* in the sense that assumptions regarding the starting atomic configuration were made or that the potential functions were semi-empirical. Recently, however, a completely *ab initio* investigation of the structure of a grain boundary in germanium (4) was made using the molecular dynamics simulated annealing method (5,6). This method allows global minimisation of the boundary energy to be achieved with respect to all electronic and ionic structural degrees of freedom using *ab initio* local pseudopotentials. The method has significant advantages in computational speed and storage requirements over traditional total energy techniques, especially when systems of low symmetry are involved or in which large relaxations take place (7).

In this paper, we present further analysis of our molecular dynamics calculations of the $\Sigma=5$ (001) twist boundary in germanium (4) using the simulated annealing approach. In particular, a calculation of the valence electron charge density in the neighborhood of each boundary state has been made to determine the exact nature of the local interatomic bonding. Experimentally, the atomic structure of various *tilt* boundaries in germanium has been deduced (8) but, unfortunately, no microscopic observations of the structure of the $\Sigma=5$ twist boundary are available. It is hoped, therefore, that the present study will stimulate new experimental interest in germanium twist boundaries.

⁽¹⁾Present address : Cavendish Laboratory, Cambridge, CB3 0HE, Great-Britain

The unrelaxed atomic configurations for the $\Sigma 5$ $1/20\langle 210 \rangle$ and $\Sigma 5^*$ $1/10\langle 210 \rangle$ boundaries are shown in Fig. 2(a,b) and their relaxed counterparts in Fig. 2(c,d). In the figures, bonds are drawn between all pairs of atoms that are separated by distances less than 1.15 times the bulk bond length (i.e., 2.7\AA). Although this cutoff distance was originally chosen arbitrarily (4), a calculation of the electronic charge density along all the bonds has shown that it is actually appropriate, as illustrated in the following section. Both relaxed structures exhibit a number of interesting features. Fig. 2(c) shows that the relaxed $\Sigma 5$ $1/20\langle 210 \rangle$ structure has perfect

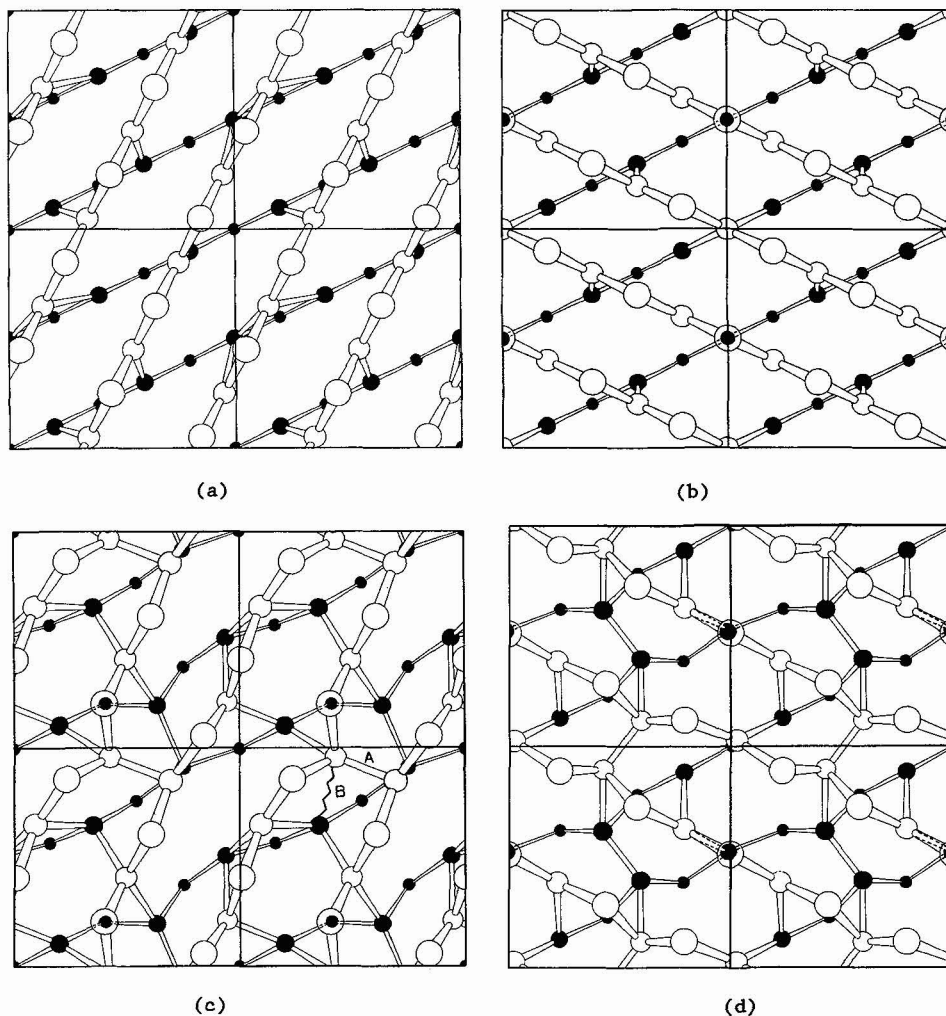


Fig. 2. Atomic positions in the two (004) planes either side of a twist boundary in germanium. Filled and open circles represent atoms in the lower and upper crystal, respectively. Four CSL unit cells are shown in each case: (a) Unrelaxed $\Sigma 5$ $1/20\langle 210 \rangle$ state, (b) Unrelaxed $\Sigma 5^*$ $1/10\langle 210 \rangle$ state, (c) relaxed $\Sigma 5$ $1/20\langle 210 \rangle$ state, (d) relaxed $\Sigma 5^*$ $1/10\langle 210 \rangle$ state.

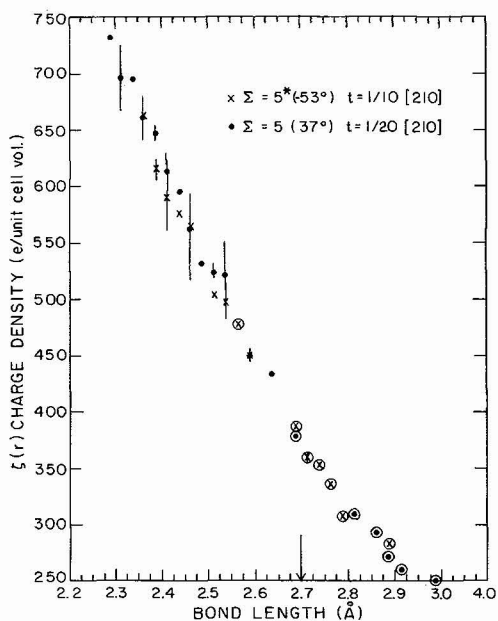


Fig. 3. Variation of valence electron charge density, at the midpoint of each bond in the core structure of the two twist boundaries shown in Fig. 2(c,d).

(12) and experimental observations (13) indicate 5, 6, 7 and 8-membered rings and four-fold coordination.

4. Charge Density Results and Discussion - The variation of valence electron charge density at the midpoint of each bond in the core region of the two twist boundary structures is summarized in Fig. 3. Bonds between pairs of atoms up to 3\AA apart have been considered (i.e., 1.28 times the bulk bond length). The range of bond lengths is divided into 0.025\AA intervals and each plotted point is an average midpoint charge density for bonds within that interval. The vertical bars represent the spread of charge density in the interval. It is seen that the data for both boundaries behave in virtually the same way, i.e., the charge density at the bond midpoint decreases linearly with increasing bond length. A decrease in charge density along a bond is, of course, expected as the bond becomes longer and weakens. Most of the data points in Fig. 3 represent cases where the variation of charge density along a bond passes through a single maximum at about the bond midpoint. Relatively strong bonds in both the bulk and at the grain boundary exhibit this behavior since the bond midpoint is where most of the valence electrons are expected to concentrate. However, some of the data points, which are shown circled, are cases where the single maximum in charge density along a bond has split into two subsidiary maxima. This occurs when a bond length is long and clearly indicates a weakened or broken bond since the subsidiary maxima can now be associated with the valence electron charge density of the individual atoms. The arrow on the abscissa of Fig. 3 indicates the bond cutoff distance used in our earlier work (4) and in drawing Fig. 2. It is seen that most of the circled points, representing weak or broken bonds, fall outside the cutoff

four-fold coordination and contains two four-membered rings per unit CSL cell. In contrast, Fig. 2(d) shows that the $\Sigma 5^{*}1/10 \langle 210 \rangle$ structure has four atoms per unit cell that have only three-fold coordination and the structure contains no four-membered rings. A characteristic of this structure is the dimers that bond across the interface to form continuous chains of four-fold coordinated atoms lying parallel to $\langle 310 \rangle$. Although not apparent in Fig. 2(c,d), both relaxed structures also involve a significant local dilation at the interface.

The detailed bonding geometries described above can be verified by mapping the valence electron charge density which is a quantity automatically determined in the present calculations. The distribution of charge density along a bond will determine its relative strength and if it is broken. This is important since Fig. 2 indicates features such as four-membered rings and three-fold coordinations which are structural elements not usually considered present in grain boundaries. In germanium tilt boundaries, for example, empirical calculations

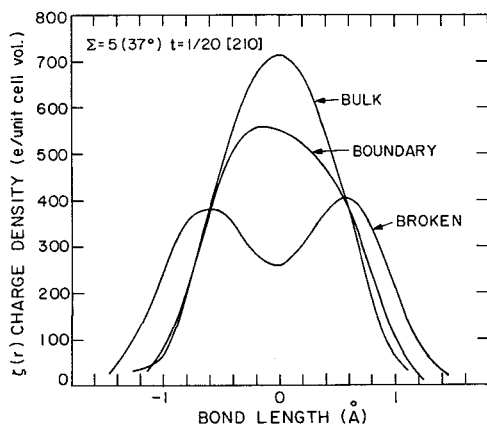


Fig. 4. Variation of valence electron charge density along a typical bulk bond, grain boundary bond and broken bond in the $\Sigma 5$ $1/20\langle 210 \rangle$ structure. The grain boundary and broken bonds are labelled A and B, respectively, in Fig. 2(c).

distance indicating that it is an appropriate choice. The three points that lie inside the cutoff distance have a charge density distribution which has barely split into two maxima and can therefore still be considered bona fide bonds.

The variation of charge density along a typical bulk bond, grain boundary bond and broken bond is shown in Fig. 4. The curves refer to bonds in the $\Sigma 5$ $1/20\langle 210 \rangle$ structure. Specifically, the grain boundary bond and broken bond are labelled A and B in Fig. 2(c). It is seen that all the curves have their expected shape with the bulk bond having the highest peak charge density. Bond B, which was a strong bulk bond before the twist boundary was formed, has now broken as illustrated by the double maxima in charge density. In comparison, bond A, which did not exist before the twist boundary was formed, is now relatively strong.

In conclusion, it has been shown that the molecular dynamics simulated annealing method for performing total energy calculations can be applied successfully to the study of grain boundary structures. In particular, the determination of the bonding geometry of two low energy twist boundaries in germanium has demonstrated the presence of intrinsic defects such as four-membered rings and three-fold coordinated atoms and this has been supported by calculating the distribution of electron charge density.

Acknowledgements - This work was supported in part by U.S. Air Force Office of Scientific Research Contract No. 87-0098 and by National Science Foundation Grant No. DMR 84-18718-A01.

References

- (1) Thomson, R. E. and Chadi, D. J., Phys.Rev. **B29** (1984) 889.
- (2) DiVincenzo, D. P., Alerhand, O. L., Schluter, M. and Wilkins, J. W., Phys.Rev.Lett. **56** (1986) 1925.
- (3) Smith, J. R. and Ferrante, J., Phys.Rev. **B34** (1986) 2238.
- (4) Payne, M. C., Bristowe, P. D. and Joannopoulos, J. D., Phys.Rev.Lett. **58** (1987) 1348.
- (5) Car, R. and Parrinello, M., Phys.Rev.Lett. **55** (1985) 2471.
- (6) Payne, M. C., Joannopoulos, J. D., Allan, D. C., Teter, M. P. and Vanderbilt, D. H., Phys.Rev.Lett. **56** (1986) 2656.
- (7) Payne, M. C. and Joannopoulos, J. D., to be published.
- (8) Grovener, C.R.M., J.Phys. C: Solid State Phys. **18** (1985) 4079.
- (9) Starkloff, Th. and Joannopoulos, J. D., Phys.Rev. **B16** (1977) 5212.
- (10) Perdew, P. and Zunger, A., Phys.Rev. **B23** (1981) 5048.
- (11) Monkhorst, H. J. and Pack, J. D., Phys.Rev. **B13** (1976) 5188.
- (12) Wetzell, J. T., Levi, A. A., Smith, D. A., MRS Proc. **63** (1986) 157.
- (13) Bourret, A. and Bacmann, J. J., Surf.Sci. **162** (1985) 495.